Trinity College Dublin
Coláiste na Tríonóide, Baile Átha Cliath
The University of Dublin

School of Physics

A Theoretical DFT study of Metal-Porphyrin derived 1-Dimensional Nano-Network Morphologies

Kevin Grainger

June 15, 2025

Submitted in partial fulfilment of the requirements for the degree of

B.A. (Mod.) Theoretical Physics

Declaration

I hereby declare that this Thesis is entirely my own work and that it has not been submitted as an exercise for a degree at this or any other university.

I have read and I understand the plagiarism provisions in the General Regulations of the University Calendar for the current year, found at `http://www.tcd.ie/calendar`.

I have also completed the Online Tutorial on avoiding plagiarism 'Ready Steady Write', located at `http://tcd-ie.libguides.com/plagiarism/ready-steady-write`.

Signed: _____ Date: _____

Acknowledgments

I would like to show my appreciation for all the help and guidance from my supervisor Prof. Cormac McGuinness. I came into the project woefully ignorant of all things physical-chemistry, I am very grateful for the resources and most importantly patience Cormac offered me. It was a privilege to work on a subsection of such an interesting project. I want acknowledge all resources and many-many CPU hours provided by Trinity High Performance Computing. Lastly I would like to Blathnait Logan for dragging my chemistry knowledge up to meet the challenge of this project.

Abstract

The following thesis is a theoretical investigation of metal-tetra-phenol-porphyrin molecules, in 1D nano-networks , both simple and novel morphologies, inspired by recent advances in porphyrin systems created via on surface synthesis [1]. The Density Functional Theory (DFT) package 'FHI-AIMS' was utilized to investigate the electronic structure and characteristics of these porphyrin networks, namely HOMO-LUMO gaps, bandstructure, electron density, density of states, exciton dynamics, absorption spectra, and magnetic interactions. This thesis is structured by morphology, each section investigating the characteristics of a new porphyrin network and it's composite parts. Namely 1D porphyrin chains, factionalized porphyrin infused graphene nano-ribbons, and finally 2D-porphyrin lattices. First the network unit cell was simulated, then the full periodic network.
It was found that the addition of the dehydrogenated phenol ligands, widened the bandgaps of the porphyrin molecules. Despite this the electronic transport properties were very promising. It was found that the 1D networks, especially the factionalized GNRs, showed spin dependant conduction properties. By fixed the spin by means of magnetic field or on metal ligands, the electronic properties changed vastly. These networks showed promised for chemical sensing applications or molecular switches.

Contents

Nomenclature

DFT	Density Functional Theory
TDDFT	Time Dependent Density Functional Theory
TPP	Tetra-Phenol-Porphyrin
DPP	Di-Phenol-Porphyrin
M-TPP	(Metal element symbol)-Tetra-Phenol-Porphyrin
M-DPP	(Metal element symbol)-Di-Phenol-Porphyrin
M-P	(Metal element symbol)-Porphyrin
Plain Metal Porphyrin	Metal Porphyrin molecule with no ligands (porphyene)
Weakly Linked Network	TPP molecules linked by only one carbon bond.
Strongly linked Network	TPP molecules linked by three carbon bonds by addition of two carbons.
Extra Strongly linked networks	TPP molecules linked by three carbon bonds by addition of two carbons.
HOMO-LUMO gap	Energy difference (eV) between the Highest Occupied Molecular Orbital (HOMO) and the Lowest Unoccupied Molecular Orbital (LUMO). m^*_{eff}
XC functional	Exchange-Correlation Functional

Effective Electr

Chapter 1

Introduction

As on-surface synthesis of more complex porphyrin-based molecules becomes possible as the field advances, there is now more space for further theoretical studies on increasing complex and novel molecular structures. These system can be investigated theoretically using DFT code packages to numerically solve the Schrödinger Equation for these many body systems. This study uses the Fritz Haber Institute ab initio simulations (FHI-AIMS) package.
This investigation builds off the previous studies, which laid the ground work for the study of large systems porphyrin systems[2]. It investigates many potential morphologies of porphyrin molecule networks, specifically using the Dehydrogenated-Tetra-Phenol-metal-Porphyrin as the unit cell. These molecules are studied along parameters that prove their useful application or the need for further study. This is achieved via the study the near Fermi-level electron structure and properties. Namely band-structure, density of states (DOS), orbital structure,charge distribution, exciton dynamics, spin channel conductance, and magnetic interaction. Given the highly theoretical nature of the project I want to give a detailed background on the mathematics used to calculate these results and draw conclusions. Additionally due the outsourcing of most calculations to the program FHI-AIMS, I want to provide the operational mathematics of the program to better allow for clearer interpret the results, and so as to not treat the DFT program as a magical 'black box'.
Each Chapter will begin with background phenomena pertinent,which shall be omitted from this Introduction section for brevity.

1.0.1 Background to the Porphyrin Molecule

Porphyrin is a large, planar, macrocyclic (large, ring-shaped) molecule composed of four nitrogen atoms symmetrically arranged within a central ring. These nitrogen atoms are embedded in four smaller carbon-based pyrrole rings, which together form the overall porphyrin structure. The core can coordinate a metal ion, resulting in a metal porphyrin, which plays a crucial role in various biological and catalytic systems. See Figure 1.
The porphyrin molecule has garnered significant interest due to its remarkable electron and energy transfer properties, which are also observed in nature, notably in chlorophyll (Magnesium-Porphyrin) and haemoglobin (Iron-Porphyrin). These properties arise from the delocalized π-electron system within the molecule, which plays a key role in its ability to facilitate efficient electron movement. The addition of transition metals to the

porphyrin structure creates a family of compounds with a range of magnetic, semiconducting, and metallic properties. The metal centre can significantly alter the electronic structure and reactivity of the porphyrin, allowing for tunable behaviour such as spin polarization, charge transfer, and the ability to conduct or store energy. These metal-porphyrin complexes have become critical in a variety of fields, from catalysis (where they mimic biological processes like oxygen transport) to electronic devices and sensors, due to their versatile electronic properties and planar stable geometry.
Atomic structure of Free Base porphyrin

1.1 Mathematical Background to Density Functional Theory

This is a theoretical study using density functional theory, This theory has allowed us to find numerical and approximate solutions to the Schrödinger equation for complex many body quantum systems (such as a large molecule) by taking electron density as the central variable to solve for. Here I will give a mathematical overview of the quantum mechanics and mathematics involved in these simulations. This will give the context needed to interpret the results in later sections.

1.1.1 The Energy Functional

A functional is a type of function. The exact definition depends on the field, but in our case: A functional takes a function as its argument and returns a number. We are effective mapping a 'vector space' on to a field of real and complex numbers. To illustrate this, take the functional I (a set of functions), this is a mapping between I and real numbers $I[f(x_0)] \rightarrow \mathbf{R}$. For example:[3]

$$I[f] = \int f(x)dx$$

DFT is concerned with the Energy functional, with electron density function as its input, returning a number which corresponds to the system energy. We are mainly using definite integral functionals.

$$E[\rho(r)] = \int H(\rho(r), \nabla\rho(r), ...)\mu(dr)$$

Where H is the energy density function, over the volume element $d\mu(dr)$. These map a function to a real number, total energy. The energy functional can also be broken down as such:

$$E(\rho(\vec{r})) = T[\rho(\vec{r})] + V_{ext}[\rho(\vec{r})] + J[\rho(\vec{r})] + E_{xc}[\rho(\vec{r})]$$

Where T is the kinetic energy functional, V_{ext} is the external potential functional, J is the Coulomb energy functional, and E_{xc} is the exchange-correlation functional. This equation is the foundation of Density Functional theory, and will be broken down further over the next view sections. In order to find ground state energy of our various systems, we need to be able to minimize our energy functional($\delta E = \int \frac{\delta E}{\delta n(\vec{r})} h(\vec{r})\, d\vec{r}$). This can be illustrated this using calculus of variations: See Appendix A1. In later sections we will also use Lagrange multipliers to find functional extrema given constraints we will encounter later on.

1.1.2 Many Body Electronic Schrödinger Equation

In our case we will mainly focus on the non-relativistic Schrödinger Equation.

$$i\frac{\partial}{\partial t}\Psi(r,t) = \hat{H}\Psi(r,t) \tag{1}$$

In our case we are considering a largely static system, therefore we will be focusing on the time dependent part of this equation. Taking $\Psi(r,t) = \phi(r)\psi(t)$, we can separate the time and spatial dependent parts.

$$i\frac{d\Psi}{dt} = E\Psi(t) \tag{2}$$

$$\hat{H}\phi(r) = E\phi(r) \tag{3}$$

We will be focusing on the latter equation [4], the TISE, to find the ground state of our systems.

Our molecule system results in a very complex Hamiltonian and thus a complex Schrödinger equation. We can describe the interactions within our system as such:

$$H = \sum_{i=1}^{N}\frac{1}{2}\nabla_i^2 - \sum_{A=1}^{M}\frac{1}{2M_A}\nabla_A^2 - \sum_{i=1}^{N}\sum_{A=1}^{M}\frac{Z_A}{r_{iA}} + \sum_{i=1}^{N}\sum_{j>i}^{N}\frac{1}{r_{ij}} + \sum_{A=1}^{M}\sum_{B>A}^{M}\frac{Z_A Z_B}{R_{AB}} \tag{4}$$

Here I used the standard notation where; A,B count over nuclei and i,j count over electrons. The first term represents electron kinetic energy, the second term is nuclei kinetic energy, the third term is coulomb attraction between nuclei and electrons, the fourth term is the coulomb repulsion between electrons, and the final term is the repulsion between nuclei.
We can separate the nuclear and electronic components:

$$\Psi([r_{i,j}],[R_{A,B}] = \Psi_{elec}([r_{ij}],[R_{AB}])\phi_{nuc}([R_A]) \tag{5}$$

Assuming slow moving nuclei, we can use the Born-Oppenheimer approximation. We can now have a Hamiltonian describing stationary nuclei with moving surrounding nuclei.
We can now remove the second term (nuclei kinetic energy) and consider the last term (nuclei repulsion) constant. This constant is also ignored as it will not contribute to the eigen-fuctions, only the eigenvalues. We end up with only an energy correction as such:

$$E_{tot} = E_{elec} + \sum_{A=1}^{M}\sum_{B>A}^{M}\frac{Z_A Z_B}{R_{AB}} \tag{6}$$

So we can now focus on the electronic Schrödinger equation.

$$H_{elec}|\Psi_{elec}\rangle = E_{elec}|\Psi_{elec}\rangle \tag{7}$$

Where:

$$H_{elec} = -\sum_{i=1}^{N}\frac{1}{2}\nabla_i^2 - \sum_{i=1}^{N}\sum_{A=1}^{M}\frac{Z_A}{r_{iA}} + \sum_{i=1}^{N}\sum_{j>i}^{N}\frac{1}{r_{ij}} \tag{8}$$

This TISE equation can only be solved analytically in very specific and simply systems. This is the where approximate DFT methods can be used to approximately find the ground state using the Variational Theorem.

$$E_{ground} = \langle\Psi_0|\hat{H}|\Psi_0\rangle \leq \langle\Psi|\hat{H}|\Psi\rangle \tag{9}$$

1.1.3 Density Functional Theory

[4]The Hartree-Fock was the first method for dealing with large many body systems, but it does not materialize in a computationally reasonable form (See Appendix) These issues are mended to an extent with Density Functional Theory (DFT). DFT poses to break down the complex TISE, much like Hartree Fock, but instead using electron density $\rho(r)$. The concept arises with the realization that the coulomb (K) term in the Hartree Fock can be approximated as:

$$E_H[n(\vec{r})] = \frac{1}{2}\int\int \frac{n(r_1)n(r_2)}{|r_1 - r_2|}dr_1 dr_2 \tag{10}$$

We are redefining the Coloumb energy at each point as the interaction of the given electron densities at each point. This energy is a function defined on a domain of functions (a functional). Electron density is a good metric to use as it contains information such as charge and thus energy and forces, while involving less variables (3 spatial variables instead of 3N), while also having to obey the physical reasonable constraints.

$$n(r) \geq 0 \tag{11}$$

$$\int n(r)dr = N \tag{12}$$

We will be focusing on Kohn-Sham DFT governed by the Hohenberg-Kohn Theorems and other approximations, using these it will be possible to estimate the ground state energy of complex systems with electron density defined as such:

$$n(\vec{r}) = N\int ...\int |\Psi(x, x_2, ...x_N)|^2 d\sigma dx_2 ...dx_N \tag{13}$$

Where integrating over $d\sigma$ will sum over the two values of spin.

1.1.3.1 Hohenberg-Kohn Theorems

[5][6]The Hohenberg and Kohn theorems are the pillars of DFT. I will outline and briefly prove each one.

Theorem A: *The external potential $V_{ext}(r)$ is uniquely determined by the ground state particle density $n(\vec{r})$, to within a constant.*
This theorem is asserting that electron density determines V_{ext} and hence fixes $\hat{H}$. And thus, all the observables are determined uniquely by the electron density $n(\vec{r})$.

Theorem B: *An energy functional E[n] exists, such that the exact ground state energy is given by the global minimum of E[n], and the ground state density is the density that minimizes E[n].*
This is an equivalent to the variational theorem, but applied to an electron density defined system. We can state that for a trial $n(r)$ (that satisfies the conditions above [39][40]) , the energy it yield will be an upper bound to the true ground state energy E_0. This allows us to 'search' for our ground state energy, as with any other quantum system.

See Appendix A3 for proofs.

1.1.3.2 Kohn-Sham DFT

Even with the Hohenberg-Kohn theorem, and with the approximate transformation of energy terms into terms involving electron density (below), there is still a need for further refinement of the theory. The next step is found in mimicking the Hartree Fock approach (non-interacting system of electrons in a mean field).

$$E_{non-int}[n] = T_{non-int}[n] + \int V_{ne} n(r) dr^3 \tag{14}$$

Interactions now can be written in one electron operators $h(r_i)$:

$$h(r_i)\psi_k(r_i) = \epsilon_k \psi_k(r_i) \tag{15}$$

And from here incorporate electron density.

The Kohn-Sham Approach to the Total Energy Functional:

The Kohn-Sham method is based on the idea of replacing the many electron interacting system with an equivalent non-interacting system. This non-interacting system should designed to reproduce the ground state energy of the interacting electron system, by constructing the correct effective potential.
Kohn Sham proposed the splitting of the F[n] term:

$$F[n] :\rightarrow T_{non-int}[n] + E_H[n] + E_{xc}[n]$$

Where $T_{non-int}[n]$ is the kinetic energy of a non-interacting system (which is known exactly), $E_H[n]$ is the Hartree energy, and E_{XC} is the exchange energy. We have imposed what is called the Kohn-Sham ansatz:

$$n(r) = 2\sum_{i=1}^{N/2} |\phi_i(r)|^2 \tag{16}$$

The wavefunctions of our non-interacting systems $\phi_j(r)$ reproduce our ground state density. These are called Kohn-Sham orbitals, and we can show that operating using these still provides a simplification in finding the ground state.

$$\begin{aligned}
E_0 &= \min_n \left\{ F[n] + \int v_{ext}(r)\, n(r)\, dr \right\} \\
&= \min_n \min_{\Phi \to n} \left\{ \langle \Phi | \hat{T} | \Phi \rangle + E_H[n] + E_{xc}[n] + \int v_{ext}(r)\, n(r)\, dr \right\} \\
&= \min_n \min_{\Phi \to n} \left\{ \langle \Phi | \hat{T} + \hat{V}_{ext} | \Phi \rangle + E_H[n_\Phi] + E_{xc}[n_\Phi] \right\} \\
&= \min_\Phi \left\{ \langle \Phi | \hat{T} + \hat{V}_{ext} | \Phi \rangle + E_H[n_\Phi] + E_{xc}[n_\Phi] \right\}.
\end{aligned}$$

Minimizing out Kohn-Sham wavefunction will yield our ground state electron density, see [48]. Now we can begin explicitly writing our total energy functional[7].

$$V_{ee} \rightarrow E_H[n] = \int\int \frac{n(\vec{r})n(\vec{r}')}{|\vec{r}-\vec{r}'|}d^3rd^3r'$$
$$F[n] = \langle\Psi|\sum_i \frac{\nabla_i}{2}|\Psi\rangle + \int\int \frac{n(\vec{r})n(\vec{r}')}{|\vec{r}-\vec{r}'|}d^3rd^3r' + E_{XC}[n]$$

Our total energy functional will look as such:

$$E[n] = T_{non-int}[n] + E_H[n] + E_{xc}[n] + \int d^3rV_{ext}(\vec{r})n(\vec{r}) \tag{17}$$

We can differentiate with respect to electron density in order to find the potential energy representation of out functional, to construct eigenvalue equations. We can state the form $V_{non-int}$ must take to replicate our interacting system

$$V_{non-int}[n(\vec{r})] = V_{ext}(\vec{r}) + V_H[n(\vec{r})] + \frac{\delta E_{xc}[n]}{\delta n(\vec{r})} \tag{18}$$

To exactly locate out ground state we must minimize our total energy functional. We can minimize the total energy functional using Lagrange multipliers and enforcing orthogonal wavefunctions as in the Hartree Fock section. To make out lives easier we can leave the kinetic energy functional $T_{non-int}[n]$, and the external potential V_{ext} in integral form.

$$E[\phi_i, n] = \langle\Phi|\hat{T}+\hat{V}_{ext}|\Phi\rangle + E_H[n_\Phi] + E_{xc}[n_\Phi] = \sum_{i=1}^{N}\int \phi_i^*(r)(-\frac{1}{2}\nabla^2 + v_{ext}(r))\phi_i(r)dr + E_H[n_\phi] + E_{xc}[n_\phi]$$

$$\frac{\delta\mathcal{L}}{\delta\phi^*(r)} = (-\frac{1}{2}\nabla^2 + v_{ext}(r))\phi_i(r) + \frac{\delta E_{\mathrm{H}}[n]}{\delta\phi_i^*} + \frac{\delta E_{\mathrm{xc}}[n]}{\delta\phi_i^*} - \epsilon_i\phi_j(\mathbf{r}) = 0 \tag{19}$$

The constrain derivative is trivial. The chain rule is used to calculate the last two functional derivatives.See Appendices for functional derivatives.

$$\frac{\delta(E_H[n] + E_{xc}[n])}{\delta\phi_i^*} = \int \frac{\delta(E_H[n] + E_{xc}[n])}{\delta n(r)}\frac{\delta n(r)}{\delta\phi_i^*}dr = (v_H + v_{ex})\phi_i(r)$$

Where we used $\frac{\delta n(r)}{\delta\phi_i^*} = \phi_i(r)$, and note that $\frac{\delta E_{xc}[n]}{\delta n(\vec{r})} = V_{xc}$

$$\left[-\frac{1}{2}\nabla^2 + v_{\mathrm{ext}}(\mathbf{r}) + \int d^3r'\frac{n(\mathbf{r}')}{|\mathbf{r}-\mathbf{r}'|} + v_{\mathrm{xc}}(\mathbf{r},[n])\right]\psi_j(\mathbf{r}) = \epsilon_j\psi_j(\mathbf{r}) \tag{20}$$

We have now arrived at the Kohn-Sham equations, which can be solved using the self consistency cycle described in Section [1.3]. But we still have no information on the form of the Exchange correlation functional.[9]

1.1.4 Exchange Correlation Functions

The exchange correlation functional is seen as representing all of the quantum interactions explicitly omitted from the Columb and kinetic terms (namely exchange

and correlation interactions), $E_{xc}[n] = E_x[n] + E_c[n]$. The form of this term is largely unknown, finding an accurate choice E_{xc} is the main issue of modern DFT calculations. A starting point for estimating this term uses the homogenous electron gas, for which the exact exchange term is know. We can used this as the basis for E_{xc} for other systems. This approach uses what is called the local density funciton.

$$E_{xc}^{\mathrm{LDA}} = \int n(\vec{r}) \varepsilon_x^{\mathrm{homo}}(n)\, dr$$

Where $\epsilon_{xc}^{homo} = \frac{-e^2}{4\pi\epsilon_0}\frac{3}{4}\frac{3n}{\pi}^{1/3} = -C_x n^{1/3}$.
As shown above, we can differentiate this term to find the exchange potential, and thus solve our Kohn-Sham eigenvalue equation.
LDAs offer a good starting point, but they assume a spatially uniform electron density, they struggle with systems of rapidly varying densities. They can often overestimate bonding energies, as atomic bonds have increased electron densities and thus increases electron-electron repulsion.

1.2 Practical DFT Calculations & Algorithmic Framework of FHI-AIMS

1.2.1 Definition of NAO basis functions

To solve the single particle Kohn-Sham equations, we must expand our single-electron wave function in terms a choose basis set. This enables us to transform our integral based Schrödinger Equations, into sums and matrix representations.
NAOs are basis functions constructed by numerically solving a radial Schrödinger-like equation. In this equation, the basis functions are defined as

$$\left[-\frac{1}{2}\frac{d^2}{dr^2} + \frac{l(l+1)}{r^2} + v_i(r) + v_{\mathrm{cut}}(r)\right] u_i(r) = \varepsilon_i\, u_i(r),$$

The function $u_i(r)$ represents the radial part of the ith basis function, where r is the radial coordinate and l is the angular momentum quantum number, determining the angular behavior. The function is influenced by $v_i(r)$, the main potential (e.g., the self-consistent free-atom potential $v_{\mathrm{free}}(r)$), and $v_{\mathrm{cut}}(r)$, a smooth confining potential that ensures $u_i(r)$ decays to zero beyond a cutoff radius r_{cut}. The eigenvalue ε_i corresponds to $u_i(r)$, defining its energy level.[8]

Wavefunction Expansion
The wavefunctions $\psi_i(\mathbf{r})$ are expanded as a linear combination of basis functions:

$$\psi_i(\mathbf{r}) = \sum_\mu c_{i\mu}\phi_\mu(\mathbf{r}), \tag{21}$$

Where: $\phi_\mu(\mathbf{r})$ are the basis functions. $c_{i\mu}$ are the expansion coefficients, which need to be determined.

Transforming the Kohn-Sham Equation into a Matrix Form
Substituting the basis expansion into the Kohn-Sham equation:

$$\hat{H} \sum_{\mu} c_{i\mu} \phi_{\mu}(\mathbf{r}) = \varepsilon_i \sum_{\mu} c_{i\mu} \phi_{\mu}(\mathbf{r}). \tag{22}$$

Now, projecting both sides onto a basis function $\phi_{\nu}(\mathbf{r})$ and integrating:

$$\int d^3r \, \phi_{\nu}^*(\mathbf{r}) \hat{H} \sum_{\mu} c_{i\mu} \phi_{\mu}(\mathbf{r}) = \varepsilon_i \int d^3r \, \phi_{\nu}^*(\mathbf{r}) \sum_{\mu} c_{i\mu} \phi_{\mu}(\mathbf{r}). \tag{23}$$

Rearranging gives the generalized eigenvalue equation:

$$\sum_{\mu} H_{\nu\mu} c_{i\mu} = \varepsilon_i \sum_{\mu} S_{\nu\mu} c_{i\mu}. \tag{24}$$

The Hamiltonian matrix elements are given by:$H_{\nu\mu} = \int d^3r \, \phi_{\nu}^*(\mathbf{r}) \hat{H} \phi_{\mu}(\mathbf{r})$. The overlap matrix elements are given by:$S_{\nu\mu} = \int d^3r \, \phi_{\nu}^*(\mathbf{r}) \phi_{\mu}(\mathbf{r})$. If the basis functions are orthonormal (e.g., plane waves), then $S_{\nu\mu} = \delta_{\nu\mu}$, and the equation simplifies to a standard eigenvalue problem:

$$\mathbf{H}\mathbf{c}_i = \varepsilon_i \mathbf{c}_i. \tag{25}$$

However, in many cases (e.g., Gaussian-type orbitals), $S_{\nu\mu} \neq \delta_{\nu\mu}$, leading to a generalized eigenvalue problem:

$$\mathbf{H}\mathbf{c}_i = \varepsilon_i \mathbf{S}\mathbf{c}_i. \tag{26}$$

This must be solved using numerical diagonalization techniques.
.

1.2.2 The Self-Consistent Field Method & Algorithm

This refers to the method used by computers to solve the Kohn-Sham equations.
The self-consistent field (SCF) equations are a set of equations that arise in mean-field theories of quantum mechanics, both in the Hartree–Fock method and Kohn-Sham Density Function Theory. They are called "self-consistent" because the effective field (or potential) in which each electron moves depends on the distribution of all the electrons, which in turn is determined by the very orbitals you're trying to compute. This leaves a 'chicken-egg' dynamic that can be solved via an initial guess of the electron density $n(\vec{r})$. We proceed to guess the original orbital solution:

$$n(r) = 2 \sum_{i=1}^{N/2} |\phi_i(r)|^2$$

. We then verify if our Kohn-Sham system 'spits out' the original guess, i.e. reaching 'self-consistency. Once this occurs we know we have the correct wave-functions to describe our system.
To illustrate the self-consistent procedure, we start with an initial guess for the Kohn–Sham orbitals, $\{\phi_i^{(0)}(\mathbf{r})\}$, which defines an initial electron density $n^{(0)}(\mathbf{r})$. This density is then used to construct the effective potential,

$$v_{\text{eff}}(\mathbf{r}) = v_{\text{ext}}(\mathbf{r}) + v_{\text{H}}[n](\mathbf{r}) + v_{\text{xc}}[n](\mathbf{r}),$$

where $v_{\text{ext}}(\mathbf{r})$ is the external (nuclear) potential, $v_{\text{H}}[n](\mathbf{r})$ is the Hartree potential arising from the electron density, and $v_{\text{xc}}[n](\mathbf{r})$ is the exchange-correlation potential obtained by functionally differentiating the exchange-correlation energy $E_{\text{xc}}[n]$. This splitting of the total energy functional,

$$E[n] = T_{\text{non-int}}[n] + E_{\text{H}}[n] + E_{\text{xc}}[n] + \int v_{\text{ext}}(\mathbf{r})\, n(\mathbf{r})\, d\mathbf{r},$$

is discussed in detail in the chapter "The Kohn–Sham Approach to the Total Energy Functional." Next, we solve the Kohn–Sham eigenvalue equation,

$$\left[-\frac{1}{2}\nabla^2 + v_{\text{eff}}(\mathbf{r})\right] \phi_i(\mathbf{r}) = \epsilon_i\, \phi_i(\mathbf{r}),$$

which yields updated orbitals $\{\phi_i(\mathbf{r})\}$ and eigenvalues $\{\epsilon_i\}$. These orbitals then define a new electron density,

$$n(\mathbf{r}) = 2 \sum_{i=1}^{N/2} |\phi_i(\mathbf{r})|^2,$$

which is mixed with the previous density (e.g., $n_{\text{new}} = (1-\alpha)n^{\text{old}} + \alpha\, n$) to enhance convergence. The cycle—recalculating the effective potential from $n(\mathbf{r})$, solving the Kohn–Sham equations, and updating $n(\mathbf{r})$—is iterated until self-consistency is reached. This procedure is elaborated in the chapter "Practical DFT Calculations & Algorithmic Framework of FHI-AIMS," ensuring that the ground state density minimizes the total energy functional.

1.2.3 Periodic Calculations The Slab Model

Using Density Functional Theory (DFT) for periodic solids does not change the fundamental Kohn–Sham equations but requires additional tools to enforce periodic boundary conditions. Bloch's theorem states that in a crystal with a periodic potential $V(\mathbf{r}+\mathbf{R}) = V(\mathbf{r})$, the electronic wavefunctions can be written as

$$\psi_k(\mathbf{r}) = e^{i\mathbf{k}\cdot\mathbf{r}}\, u_k(\mathbf{r}), \quad \longrightarrow u_k(\mathbf{r}) = \sum_{\mathbf{G}} c_{k,\mathbf{G}}\, e^{i\mathbf{G}\cdot\mathbf{r}},$$

Where $u_k(\mathbf{r})$ is periodic with the lattice. Expanding $u_k(\mathbf{r})$ in a plane-wave basis and substituting into the Kohn–Sham equations transforms the problem into a matrix eigenvalue problem in reciprocal space. This approach, combined with Monkhorst–Pack grids (See Appendix) for efficient Brillouin zone sampling, enables the calculation of electronic band structures.

1.3 Electronic Structure the Porphyrin Molecule

Porphyrin is a large, planar, macrocyclic (large, ring-shaped) molecule composed of four nitrogen atoms symmetrically arranged within a central ring. These nitrogen atoms are embedded in four smaller carbon-based pyrrole rings, which together form the overall porphyrin structure. The core can coordinate a metal ion, resulting in a metal porphyrin, which plays a crucial role in various biological and catalytic systems. See Figure 1.

The porphyrin molecule has garnered significant interest due to its remarkable electron and energy transfer properties, which are also observed in nature, notably in chlorophyll (Magnesium-Porphyrin) and haemoglobin (Iron-Porphyrin). These properties arise from the delocalized π-electron system within the molecule, which plays a key role in its ability to facilitate efficient electron movement. The addition of transition metals to the porphyrin structure creates a family of compounds with a range of magnetic, semiconducting, and metallic properties. The metal center can significantly alter the electronic structure and reactivity of the porphyrin, allowing for tunable behaviour such as spin polarization, charge transfer, and the ability to conduct or store energy. These metal-porphyrin complexes have become critical in a variety of fields, from catalysis (where they mimic biological processes like oxygen transport) to electronic devices and sensors, due to their versatile electronic properties and planar stable geometry.
Atomic structure of Free Base porphyrin

1.3.0.1 Electronic Structure of the Free-Base Porphyrin

Omitting the central metal gives a free-base porphyrin, a system dominated by the carbon complex. The de-localized electrons in the porphyrin molecule are a result of carbon double bonds, which form the π-orbitals. This forms a cyclic cloud of electrons which can move with relatively greater freedom around the porphyrin molecule. This allows for exceptional electron transfer properties due to high electron mobility. Porphyrins are an aromatic molecule, aromaticity refers to the increased stability of molecules caused by de-localized electrons in conjugated rings, which lowers overall energy. A metal porphyrin structure is further stabilized by its' nitrogen atoms, which anchor the interior metal atom, allowing for predictable electronic states and electron donation. This specific electronic structure causes various physical phenomena that invite investigation.

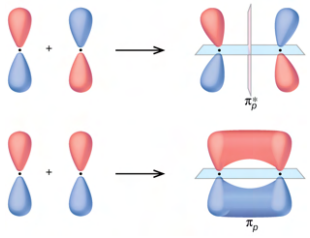

Figure 1.1: π & $\pi*$ bonding [12].

1.3.1 Metal Porphyrin Electronic Structure

The coordination of a free-base porphyrin with a metal atom significantly alters its electronic structure. The metal ion introduces new interactions with the π-electrons in the porphyrin ring, particularly through hybridization between the metal's d-orbitals and the porphyrin's π-orbitals. This interaction shifts the energy levels of the molecular orbitals, influencing the distribution of electron density across the system. The metal's d-orbitals can donate or accept electron density, altering the electronic configuration of the porphyrin, which impacts its reactivity and stability.
This study will consider only Vanadium, Manganese, Iron, Cobalt, and Zinc porphyrin. This group represents a wide spread of d-orbital occupation numbers. Thus, we expect

to see a variety of results as each metal atom has different propensities to interact with the Nitrogen and Carbon ligands due to d-shell occupation, each metal has its own spread of d-orbital energies, which will 'break-up' the HOMO-LUMO gap differently. And each metal have a variety of unpaired electron numbers, leading to differing magnetic interaction.
These specific transition metals offer a number of interesting avenues for investigation:

- Vanadium (d^3) — represents early transition metal behaviour, and is know to exist in many possible oxidation states (V^{+3}, V^{+4}, V^{+5}) depending on ligand strength.
- Iron (d^6) — Common in porphyrin systems (as Fe^{+5} and Fe^{+3}), and adaptable spin states that influence electronic and magnetic properties.
- Cobalt (d^7) — Demonstrates strong magnetic anisotropy.
- Zinc (d^{10}) — A closed-shell system with no unpaired electrons, making it diamagnetic and ideal as a non-magnetic reference in conduction or sensing studies.

To fully interpret the results of the molecular simulations, we need an understanding of the general orbital structure and orbital interactions of the porphyrin.

The Four Orbital Model The Four Orbital Model is a well accepted simplification of metal-porphyrin orbitals. The Four-Orbital Model postulates four key orbitals formed by the hybridized orbitals of the metal-porphyrins constituent parts.

- Carbon π-orbitals from the exterior ring
- Nitrogen π-orbitals from the internal atoms
- Anti-bonding π^* orbitals from the conjugation of the carbon and nitrogen atoms
- d-orbitals from the central metal atom.

These four orbitals are considered crucial in determining the electronic structure and spectral properties of porphyrins. It is important to note that this is a large simplification, and more complex hybrid orbitals exist, depending especially on the central metals' d-orbital arrangement. We pay close attention to the filling of these metal de-orbitals, as this defines how electrons move from the metal centre to the outer porphyrin or vis-versa.
To give further detail on the main constituent groups:

Bonding and Anti-Bonding π-Orbitals:
π-Orbitals are formed by the overlap of the p-orbitals of the carbons on the conjugated pyrrole rings of the porphyrin, and the carbon rings of the Tetra-Phenol arms. This results in a system a 'cloud' like system of de-localized electrons on the horizontal axis, above the planar porphyrin. Bonding orbitals are formed by the constructive interference of these p-orbitals, and occupy lower energy states. Anti-bonding π-orbitals are formed by destructive interference, they can also occur from the interference of the Nitrogen atoms on the carbon π-bonding. These occupy higher energy levels and are considered unfilled in the ground state, leaving them available for π-back-donation from the metal centre.

Nitrogen π-Orbitals:
The nitrogen atoms in the porphyrin's core each have a lone pair of electrons in Nitrogen π-orbitals that interact with the π-electron system. These nitrogen π-orbitals can overlap with the anti-bonding π^*-orbitals from the conjugated carbon rings, as these are at a higher, more accessible energy. This interaction can influence the overall electron distribution in the molecule, further stabilizing the system and enhancing electron de-localization. However, their contribution to charge bonding & charge transfer is less significant than that of the carbon π-orbitals but still plays a crucial role in maintaining the porphyrin's planar structure.

d-Orbitals from the Central Metal Atom:
The metal centre in a metal-porphyrin complex introduces a set of d-orbitals that interact with the π-electron system of the porphyrin. These d-orbitals can overlap with the anti-bonding π^*-orbitals of the porphyrin ring, enabling π-back donation where electron density is transferred from the metal's d-orbitals to the empty π^*-orbitals. This interaction significantly alters the electronic properties of the porphyrin, influencing the near Fermi-level density of states, thus altering values such as the HOMO-LUMO gap. The porphyrin-metal interaction is highly dependent on the choice of metal, as different metals have a different spread of d-orbitals at different energies and occupations. The ligand-field strength is also an important factor, as it can determine the splitting of the d-orbitals.

1.3.2 Exciton Dynamics in Metal Porphyrins

π-Back Donation The central metal can partake in π-back donation. This occur when the metal ion has d-electron available for donation to the ring of $\pi*$ orbitals (anti-bonding). This increases the degree of metal-ligand bonding.
This type of donation is dependent on the number of d-electrons available for donation, higher oxidation states tend to have fewer available d-electrons, for example. The energy levels of these d-electrons are also important, they dictate the possibility or efficiency of π back-donation, these energy levels could too disparate from that of the ligands $\pi*$-orbitals.
The Oxidation state of the metal defines much of this interaction. Lower oxidation states (less ionized, more available electrons), are more likely to back donate as their orbitals are more populated.

σ Donation The Nitrogen in the porphyrin each posses lone pairs of electrons. These are available for what is called σ-donation to an empty metal orbital. This requires the availability of low-lying metal orbitals, to form a σ-bond between metal and Nitrogen. A strong σ bond will result in a anchored, and thus more planar metal. As with *pi*-back donation, it is also dependent on oxidation state of the metal. But σ-donation tends to have less involvement with electron de-localization.

Ligand Field effects: Different ligands have differing field strengths, this has a large affect on the central metal. And will largely determine its' oxidation state, as a strong field will pull electrons off the metal, or visa-versa. Therefore, the ligands influence the oxidation state of the metal primarily by providing or withdrawing electron density, and this, in turn, affects the metal's electronic configuration and its tendency to adopt a

particular oxidation state. This can intern affect important properties; electron transfer (resulting from a change in oxidation state), and magnetism (resulting from paired or unpaired electrons). We will expect to see small effects in our own molecules and composite systems as we change the ligand structure.
Ligand field theory (LFT) is a model used to describe the behaviour of transition metal complexes, focusing on how the central metal's d orbitals are affected by the surrounding ligands. LFT also takes into account the orbital interactions (such as covalent bonding) between the metal and ligands. In the presence of ligands, the degeneracy of the metal's d orbitals is broken, causing them to split into different energy levels. This splitting is influenced by the geometry of the ligand arrangement around the metal centre. The splitting depends on the symmetry of ligands, in our case we will mainly have C4v symmetry (typical of ligands at 90 degrees) In C4v symmetry, the d orbitals split into different energy levels: $dx^2 - y^2$ (highest energy), dz^2, dxy, dxz and dyz (lowest energy).

1.3.3 Inter-Porphyrin Bonding

The structural organization of porphyrin systems plays a critical role in their collective physical properties. Figure 3 illustrates the standard bonding co-ordination of a porphyrin molecule, highlighting the regions where intermolecular interactions occur. Inter-porphyrin bonding can be mediated through several mechanisms, including:

- **Carbon Bridges:** Each porphyrin unit cell can be connected with varying number of carbon rings. The grater the number of bridging carbon rows the more graphene-like our system becomes. In this thesis porphyrin unit cells bridged with more carbons is considered a 'strongly' linked system. It is expected a strongly linked system will exhibit more graphene-like properties; greater π-orbital delocalisation, metallic behaviour, and smaller HOMO-LUMO gaps.

- $\pi - \pi$ **Stacking:** The planar nature of porphyrins facilitates strong $\pi - \pi$ interactions between the delocalized electron clouds of adjacent molecules. These non-covalent interactions not only promote the formation of ordered arrays but also influence the electronic coupling between porphyrins, which is essential for charge transport and energy transfer.

- **Metal-Ligand Bridges:** In systems where metal centres are present, bridging ligands can serve as conduits for electron exchange between adjacent porphyrins. This linkage can lead to enhanced electronic communication and the formation of extended networks, which are of interest for applications in molecular electronics.

This thesis will focus on inter-porphyrin linkages that have been completely or partially physically realized through on-surface synthesis. Emphasis will be placed on understanding how these bonding interactions influence the electronic, optical, and magnetic properties of the resulting structures, as well as their potential for device integration. See the figures below for examples of synthesized linkage motifs.

Chapter 2

Chain Simulations

2.1 Preliminary Molecular Simulations

Before diving into Metal Porphyrin networks it is necessary to start with a brief investigation into our constituent molecules, the 'jigsaw' pieces we will move forward with when creating our networks. The focus of this thesis is the cyclo-dehydrogenated tetra phenol porphyrin. This refers to larger porphyrin molecule with four phenol 'arm' , that through complex chemical steps, can be fully attached to the porphyrin sided, leading to this star shape:
There has been extensive study on the standard metal porphyrin, it has been simulated many times in many morphologies, serving as a good comparison for the TPP, with a litany of different ligands. I will include some calculations for the plain porphyrin here, but only for comparison purposes. The aim of this thesis is to show the unique characteristics found with the TPP molecule, and the many variations of linkages between unit cells.
The band structures and DOS plots we will see for more complex networks are hard to interpret without being familiar with that of the most simple unit cell. In this section we have the energy level eigenvalues, HOMO-LUMO gaps, DOS and pDOS. This section will investigate the metal ligand interactions for the unit cell.
Given the amount of lengthy-named morphologies, I will be using short hand nomenclature as follows:

- TPP - cyclo-dehydrogenated tetra phenol porphyrin
- DPP - cyclo-dehydrogenated tetra phenol porphyrin

[insert diagrams here]
We will be analyzing these molecules with the aim of better understanding the, ease charge delocalization, metal-ligand interaction, structure and stability. To achieve this, for each metal porphyrin, we will solve the Kohn-Sham eigenvalues (orbital energies), plot the orbital volume-metric data (HOMO-LUMO $\pm$ 4), a species (element) projected density of state, and a structural relaxation on conjugate porphyrin.

HOMO-LUMO Gaps The HOMO (highest occupied molecular orbital) and LUMO (lowest unoccupied molecular orbital), often referred to as frontier orbitals, play a crucial role in electron transport properties, particularly in periodic systems. The HOMO-LUMO gaps for out individual M-TPP and M-DPP molecules should give us a

good insight into their periodic counterparts. The size of these gaps can largely determine the potential application of the porphyrin, as either a semi-conductor (used in photo-voltaics and molecular electrons) or semi-metals (used for charge transport in molecular electronics).
We also need to consider the physical location of these HOMO and LUMO orbitals within the molecules. The HOMO can be thought of loosely as the donor region, and the LUMO as the acceptor.
If the HOMO is spatially extended over many atoms, the electron can be more easily delocalize, as it can move 'freely' without having to tunnel into other orbital. On the other hand if the HOMO is localised, the molecule will behave like a set of isolated regions, with their own electron densities.
The LUMO's position is important in the same way. If the LUMO is extended over several atoms, we have a wider region of acceptance for a potentially delocalised electron. For example, in $d - \pi$ orbital interactions (e.g. *pi*-back donation), the LUMO of the ligand can overlap with the HOMO of the metal, facilitating depoliticisation.
It is important not to over-state the potential for electron de-localisation, most electron-hole pairs recombine very quickly. But these orbital features can point towards features in larger systems or in the molecule under particular conditions.

2.1.0.1 Computational Details:

All simulations were run with the same parameters. Each Simulation was conducted first using the standard PBE functional. The convergence criteria where as follows:

- $\Delta n(\vec{r}) = 1E - 5$
- $\Delta E_{tot} = 1E - 5$
- Relaxation energy tolerance $= 1E - 2$

Convergence Parameters:

- Pre conditioner: Kerker 2.0
- Pulay Mixing, charge mixing parameter 0.3
- Gaussian Occupation, smearing 0.008

It was aimed to strike a balance between accuracy and computation time and cost. The Vanadium and Iron porphyrins where calculated using both spin collinear settings and no spin. Table 2.1 shows the HOMO-LUMO gaps for non-spin polarized calculations.

2.1.0.2 Orbital Energies

We will simulate Zn,Fe,V respectively. Given the focus is on the affect of the particular ligand morphology, we will order the simulations element-wise so as to ascertain the affect of the ligand structure on the metal porphyrin, not visa-versa.
Tabel 2.1 shows the HOMO-LUMO gaps for non-spin polarized calculations of the Zn, V & Fe Porphyrins. The ligand effect isn't particularly obvious, but we see a loose trend towards a smaller HOMO-LUMO gap with the larger ligands (TPP). The defining factor is expected to be the central metal, and where its' d-orbitals lie with

	Zn	Fe	V
TPP	1.141 eV	0.058 eV	0.743 eV
TPP Spin Up		0.3125 eV	0.453 eV
TPP Spin Down		0.625 eV	1.351 eV
DPP	0.0998 eV	0.028 eV	0.334 eV
DPP Spin Up		0.537 eV	0.24 eV
DPP Spin Down		0.442 eV	0.482
P	2.77 eV	0.099 eV	1.141 eV

Table 2.1: HOMO-LUMO gap sizes (in eV) for Zn, Fe, and V complexes with TPP, DPP, and P ligands.

respect to the the carbon ligand structure. The next section will examine the near fermi level energies in more detail. We see a large variation in results from the collinear simulations, from the Iron and Vanadium. Especially in the TPP configuration.

2.1.0.3 Zn-P, Zn-DPP & ZnTPP

The zinc metal has a full d shell of electrons, meaning it is not amenable to any electronic interaction with its' surrounding. This was seen in the orbital diagrams and in the density of states. There is next to no contribution from the central zinc atom. The near fermi level orbitals are carbon dominated. Notice the delocalised pi-orbitals, this level of pi-orbital de localisation is far greater than any of the other metals near fermi level. We can expect this is due to the lack of interaction between zinc orbitals and the surrounding carbons, resulting in undistributed pi-delocalisation. A 1D system using zinc as the unit cell shows potential for favourable charge carrying properties, and will serve as good contrast to the other metals.

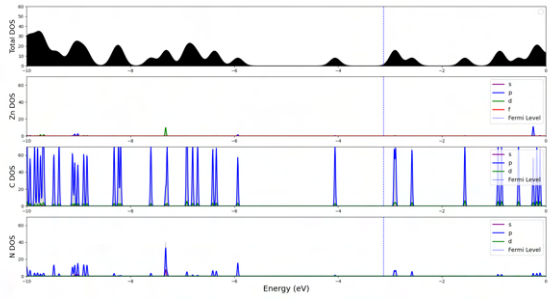

Figure 2.1: Collinear Spin Study - ZnTPP

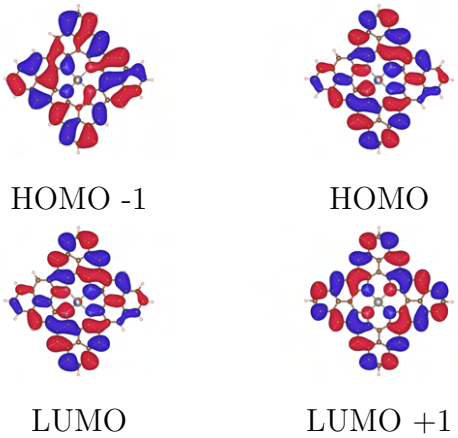

Fe-P, Fe-DPP & Fe-TPP The Iron based porphyrin units provide interesting insight. We around fermi level the Iron d orbitals contribute. The positioning of the d-orbital energy level leads to a much shortened HOMO-LUMO gap. An interesting result is found from a spin polarized calculation, we see a modulation in the HOMO-LUMO gap size in each each spin-channel.
The location of the HOMO state on the Iron metal, would imply a metal-carbon donation. This would have implication on a 1D system. The degree of hybridization

between the Fe centred HOMO and adjacent molecular orbitals could determine the transport regime—whether it follows band-like transport or hopping conduction. There is weak interaction between the Iron orbitals and the nitrogen, but we seem to have very disparate energy levels in the Iron porphyrins.

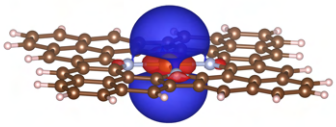

Figure 2.2: Fe-TPP HOMO (Alternate angle of Iron d_{z^2}-orbital

There is little difference seen in the Iron DPP and TPP molecules. The Iron centre of each of these molecules is seen to be in the first oxidation state, having lost 1 electron. This suggests the ligand fields are not having a large impact on the metal centre. This would lead us to believe the other transition metals will show low oxidation states also. We also see a spin state of $S = 2$, this is lower than expected, but in keeping with the oxidation state. The magnetic moment is thus $\mu = 6.9$, this would further suggest strong paramagnetism. This is promising for spin-channel dependent conduction properties. The DPP configuration yields the same oxidation and spin states, this is unusally given the change in ligand structure.

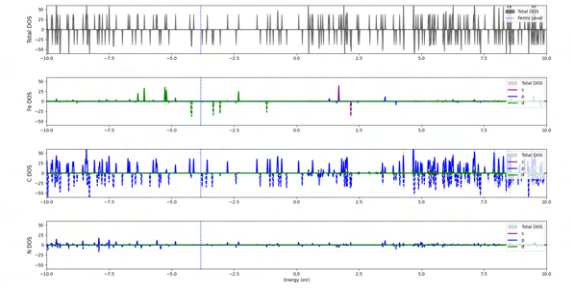

Figure 2.3: Collinear Spin Study - FeDPP

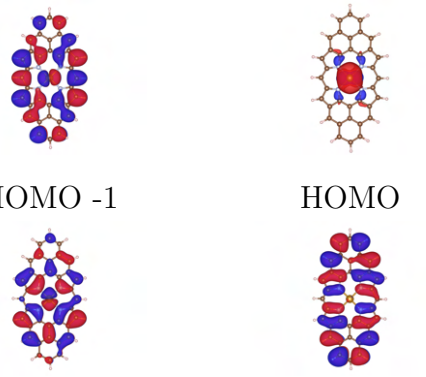

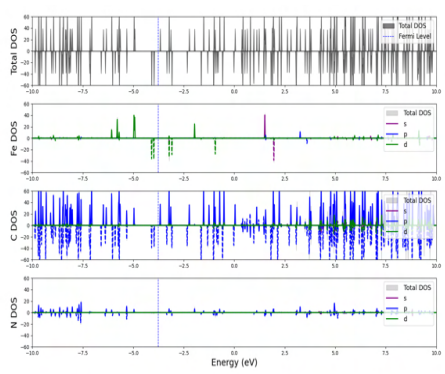

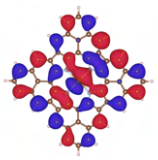

HOMO -1

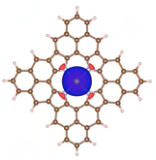

HOMO

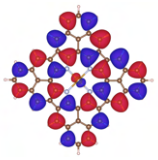

LUMO

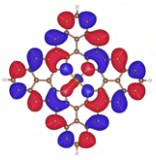

LUMO +1

Figure 2.4: Collinear Spin Study - FeTPP

2.1.0.4 V-P, V-DPP & V-TPP

The Vanadium Porphyrins show similar d-orbital behaviour to that of the Iron. The Vanadium d-orbitals' energy levels align well with that of the surrounding structure. We see a contribution and splitting of the metals orbital near the HOMO-LUMO level. The orbital is splitting along d_{xy} The system is largely carbon dominated, so we see pi-localisation.
There is a large difference in the spin-channel d-orbital distribution in Figure 2.6. The Vanadium centre appears in the first oxidation state V^{+1}, while it is is approaching a high spin state with 2.6 unpair electrons. This is the case for both DPP and TPP configurations.

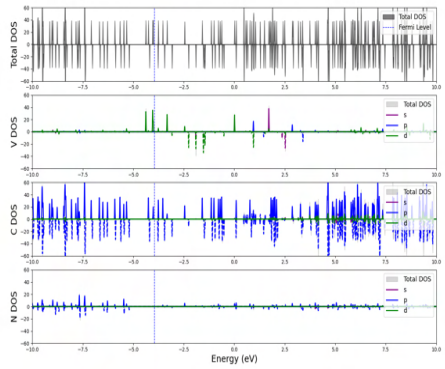

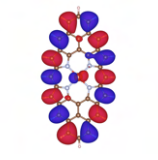

HOMO -1

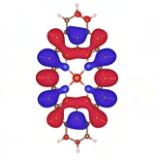

HOMO

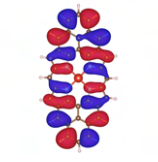

LUMO

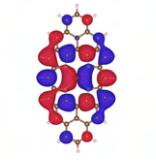

LUMO +1

Figure 2.5: Collinear Spin Study - V-DPP

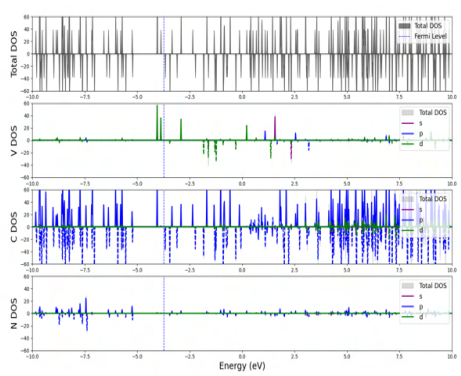

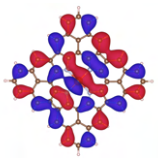

HOMO -1

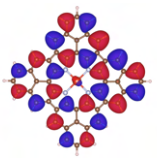

HOMO

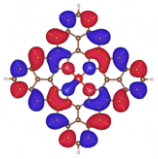

LUMO

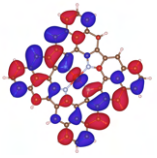

LUMO +1

Figure 2.6: Collinear Spin Study - V-TPP

2.1.0.5 Co-P, Co-DPP & Co-TPP

The analysis of the Cobalt Porphyrin has potential interest due to its' many spin states and potential for paramagnetism. I have conducted a species and orbital density of states. We ultimately see no real effect on the density of states by the cobalt centre. This could be due to effect of the axial ligands imposing a lower spin state. The graphs are included in the appendix.

Chapter 3

Chain Simulations

Now that the dynamics of the individual molecules have been investigated, this section will model 1-dimensional systems with these molecules (TPP,DPP) as the unit cell. The use of the TPP as a unit cell is over particular interest due to the apparent 'tunability' of the connection between each unit cell. Each arm of the molecule can mesh into 'graphene' like connections of carbon rings, deciding the size of this carbon connection should change characteristics of the network such as charge transfer.
I have ordered these by element, to isolate the effects of the changing ligand environment. We will approach each of these in separate sections.
As described in the introduction of the thesis, we are investigating the electronic structure near the Fermi-level. We will study charge transport and magnetic interactions.

3.0.0.1 Computational Details:

For the periodic chain calculations the above parameters where kept the same. The K-grid used was 30 x 1 x 1. This provided suitably finely sampled Bouillon zone along the chain direction. The band structure was thus sampled along the K-path $\Gamma \rightarrow X$.

3.0.0.2 Computational Details:

All simulations were run with the same parameters. Each Simulation was conducted first using the standard PBE functional. The convergence criteria where as follows:

- $\Delta n(\vec{r}) = 1E-5$
- $\Delta E_{tot} = 1E-5$
- Relaxation energy tolerance $= 1E-2$

Convergence Parameters:

- Pre conditioner: Kerker 2.0
- Pulay Mixing, charge mixing parameter 0.3
- Gaussian Occupation, smearing 0.008

Due to the shear number of simulations it would not be feasible to include them all here. I have included the most interesting chain morphologies for each transition metal.

3.0.1 Zinc Chains

The Zinc periodic calculations preform as expected. We see extensive pi-orbital de-localisation. As well as this the band gap shrinks from weak to strong coupled networks.

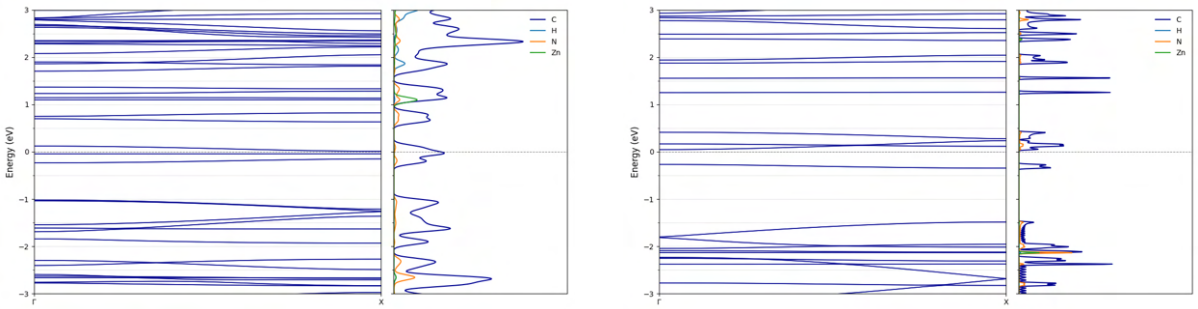

(a) Zinc Strongly Coupled (b) Zn Weakly Coupled

Figure 3.1: Comparison of Band Structures for Zinc Coupling

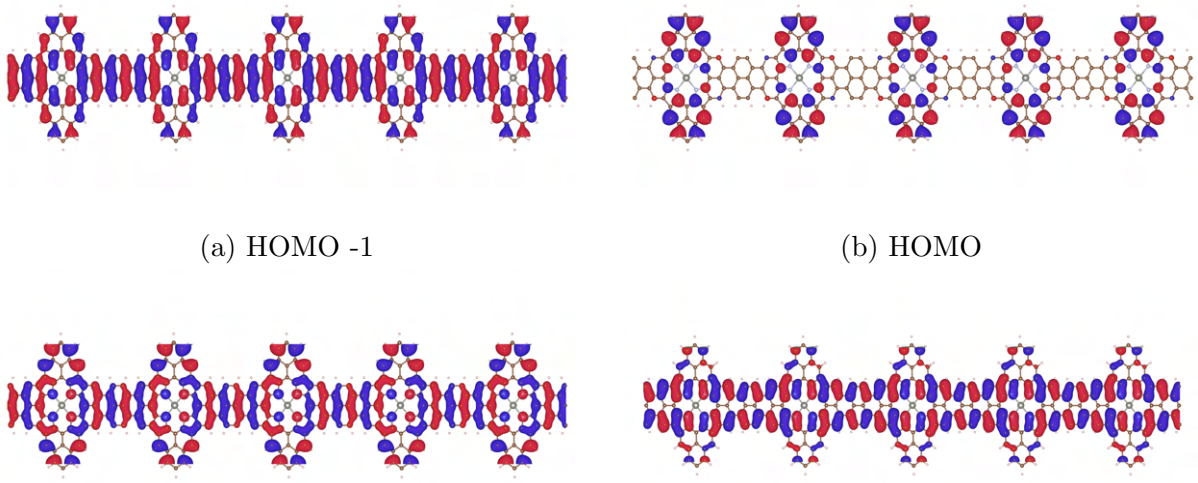

(a) HOMO -1 (b) HOMO

(c) LUMO (d) LUMO +1

Figure 3.2: Electronic States Visualization for ZnStrong Chain

3.0.2 Iron Chains

A network of particular interest is FeDPP, we see a widening of the bandgap in the Spin-down channel. As with the individual FeDPP molecule the HOMO state is dominated by the central metal, yet the LUMO is entirely carbon dominant. This could lead to metal back donation into the carbon pi* orbitals.

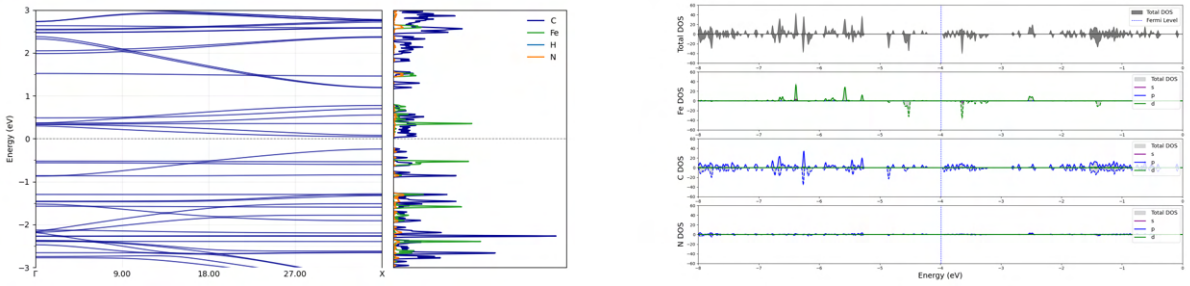

(a) Band-structure of Fe-DPP (b) PDOS Fe-DPP

Figure 3.3: Comparison of Band-structure and PDOS for Fe-DPP

(a) HOMO -1 (b) HOMO

(c) LUMO (d) LUMO +1

Figure 3.4: Electronic States Visualization for FeDPP Chain

3.0.3 Vanadium Chains

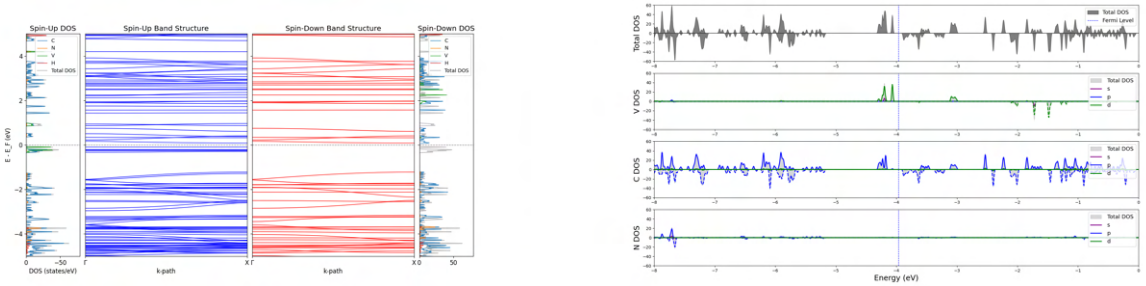

(a) Band Structure & Species Proj DOS V Weakly Coupled (b) Orbital Proj DOS by Species V Weakly Coupled

Figure 3.5: Comparison of Band Structure and DOS

I have split the bandstructure by spin channel, we see for spin up, a contribution from the Vanadium d-orbital significantly shortens the bandgap of the chain. The Periodic

configuration of the V-TPP molecule had enhanced the favourable characteristics seen in chapter 1.

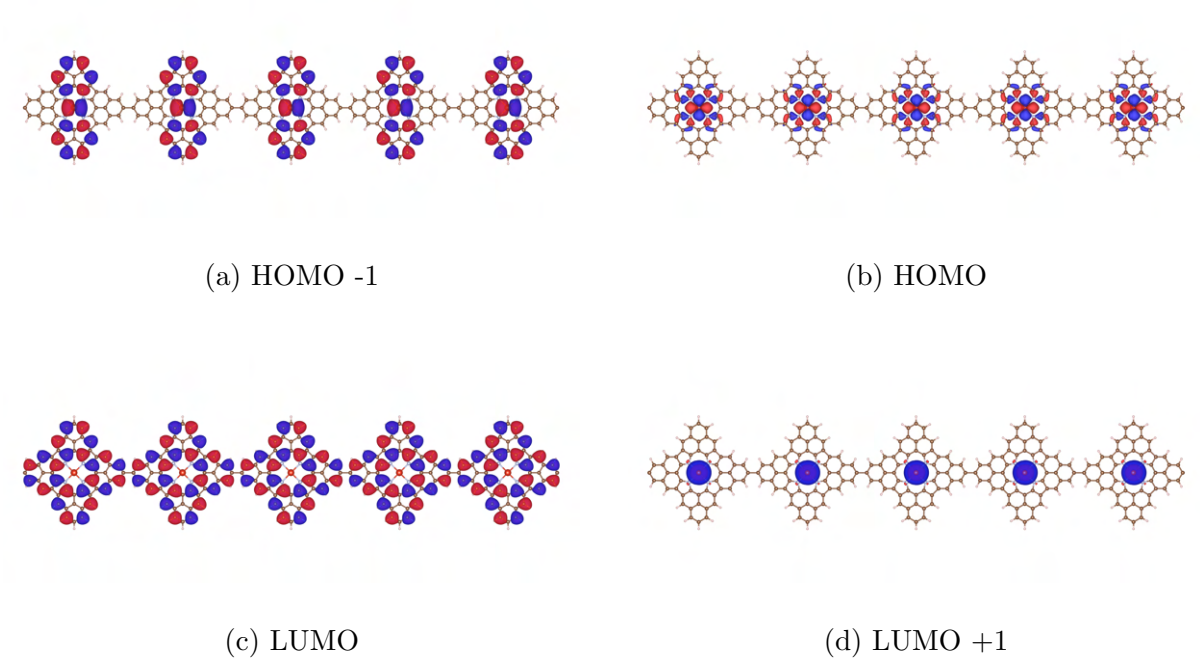

(a) HOMO -1

(b) HOMO

(c) LUMO

(d) LUMO +1

Figure 3.6: Electronic states visualization

The bandstrucuture of Weakly connect Vanadium Porphyrin varies greatly based off spin-channel. This can similar been seen in Vanadium Extra Strongly coupled. It seems the d-orbital energy levels for vanadium intersect well with the carbon energy levels around fermi level. Further more, the central metal at HOMO energy level form hydrid bonds, these chains look promising for charge conduction, and dir

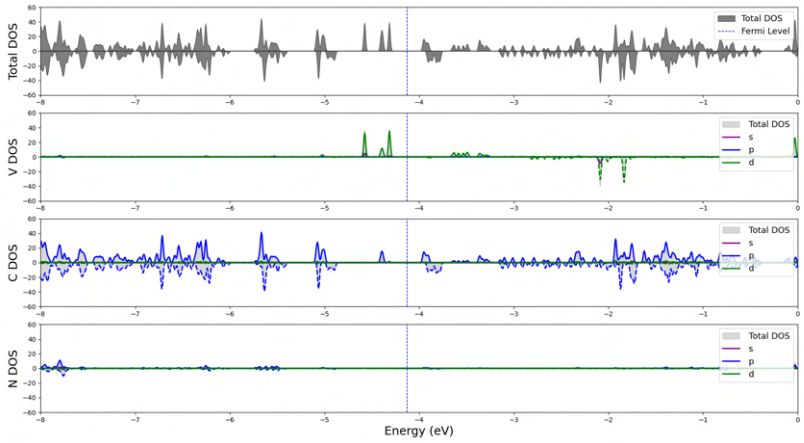

Figure 3.7: Species & Orbital Proj DOS V-Extra

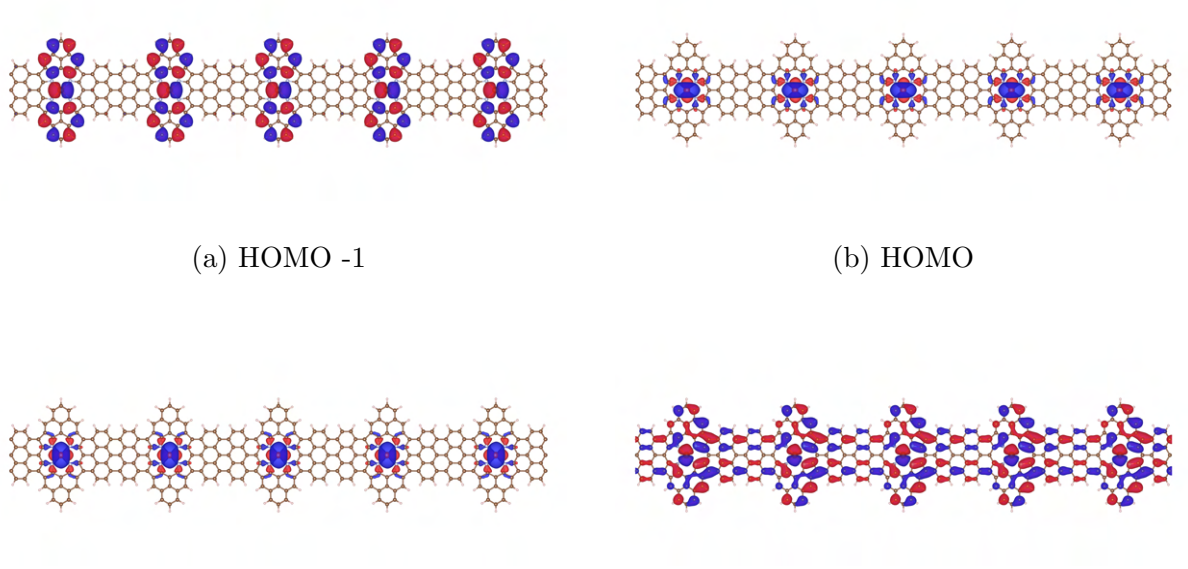

(a) HOMO -1

(b) HOMO

(c) LUMO

(d) LUMO -1

Figure 3.8: Electronic states visualization for Vextra Chain

3.0.4 Cobalt Chains

The behaviour obtained from the Cobalt chains where again slightly usual. The cobalt centre had very little impact on the chain as a whole. I believe there could have been convergence issues with the calculation, as even the carbon DOS do not align well with the other transition metal porphyrins. With more time I would conduct magnetic studies on these Cobalt porphyrins, as they do show great variation in each spin channel. I have attached the Cobalt PDOS in the Appendix.

Chapter 4

Conclusion & Discussion

4.1 Conclusions & Future Work

In Conclusion, tetra-phenol metal-porphyrins show great promise for future use in molecular electronic application. They show an ability for spin-tunable conductance. These 1D networks could have interesting applications in chemical sensing also, if a spin could be impose via on metal ligand. Furthermore, the interesting role and spatial distribution of the metal d-orbital near of fermi level, could make them useful for application where exciton dynamics are important.

Bibliography

Appendix A1

Mathematical Appendix

You may use appendices to include relevant background information, such as calibration certificates, derivations of key equations or presentation of a particular data reduction method. You should not use the appendices to dump large amounts of additional results or data which are not properly discussed. If these results are really relevant, then they should appear in the main body of the report.

A1.1 Functional Derivatives:

A functional is a type of function. The exact definition depends on the field, but in our case: A functional takes a function as its argument and returns a number. We are effective mapping a 'vector space' on to a field of real and complex numbers. To illustrate this, take the functional I (a set of functions), this is a mapping between I and real numbers. For example:

$$I[f(x_0)] \rightarrow \mathbf{R}$$

$$I[f] = \int f(x)dx$$

DFT is concerned with the Energy functional, with electron density function as its input, returning a number which corresponds to the system energy. We are mainly using definite integral functionals.

$$E[\rho(r)] = \int H(\rho(r), \nabla\rho(r), ...)\mu(dr)$$

Where H is the energy density function, over the volume element $d\mu(dr)$. These map a function to a real number, total energy. The energy functional can also be broken down as such:

$$E(\rho(r)) = T[\rho(r)] + V_{ext}[\rho(r)] + J[\rho(r)] + E_{xc}[\rho(r)]$$

Where T is the kinetic energy functional, V_{ext} is the external potential functional, J is the Coulomb energy functional, and E_{xc} is the exchange-correlation functional. This equation will be broken down further over the next view sections.

Functional Derivatives:
In order to find ground state energy of our various systems, we need to be able to minimize our energy functional. To give a short outline of the functional calculus used.

The derivative of a functional tells us how the functional changes with respect to its argument function f(x). To illustrate this using calculus of variations:
Consider a functional $I[f(x)]$ of the form:

$$I[f] = \int H(x, f(x), \nabla f(x))\, dx. \tag{1}$$

We introduce a small perturbation in the function $f(x)$ as:

$$f(x) \to f(x) + \epsilon h(x), \tag{2}$$

where ϵ is a small parameter and $h(x)$ is an arbitrary variation.
The change in I is given by:

$$\delta I = \lim_{\epsilon \to 0} \frac{I[f + \epsilon h] - I[f]}{\epsilon}. \tag{3}$$

Expanding $I[f + \epsilon h]$ in ϵ and keeping only the linear term and subbing back in the explicit functional definition:

$$I[f + \epsilon h] = I[f] + \epsilon \int \frac{\delta I}{\delta f(x')} h(x')\, dx' + O(\epsilon^2). \tag{4}$$

The quantity $\frac{\delta I}{\delta f(x')}$ is called the functional derivative, and it generalizes the concept of the gradient in function space. The functional derivative satisfies:

$$\delta I = \int \frac{\delta I}{\delta f(x')} h(x')\, dx'. \tag{5}$$

This represents the first-order variation of the functional, and the term $\frac{\delta I}{\delta f(x')}$ acts as the directional derivative at $f(x)$ in the direction $h(x)$. . In later sections we will also use Lagrange multipliers to find functional extrema given constraints we will encounter later on.
Where T is the kinetic energy functional, V_{ext} is the external potential functional, J is the Coulomb energy functional, and E_{xc} is the exchange-correlation functional. This equation is the foundation of Density Functional theory, and will be broken down further over the next view sections. In order to find ground state energy of our various systems, we need to be able to minimize our energy functional. This can be illustrated this using calculus of variations
Consider a functional $E[n(\vec{r})]$ of the form:

$$E[n] = \int H(\vec{r}, n(\vec{r}), \nabla n(\vec{r}))\, d\vec{r}. \longrightarrow \delta E = \int \frac{\delta E}{\delta n(\vec{r})} h(\vec{r})\, d\vec{r}. \tag{6}$$

The quantity $\frac{\delta E}{\delta n(\vec{r})}$ is called the functional derivative, and it generalizes the concept of the gradient in function space. The functional derivative satisfies: This represents the first-order variation of the functional, and the term $\frac{\delta E}{\delta n(\vec{r})}$ acts as the directional derivative at $n(\vec{r})$ in the direction $h(\vec{r})$. . In later sections we will also use Lagrange multipliers to find functional extrema given constraints we will encounter later on.

A1.2 Proof of the Hohenburg-Kohn Theorems:

A1.2.0.1 Hohenberg-Kohn Theorems

The Hohenberg and Kohn theorems are the pillars of DFT. I will outline and briefly prove each one.

Theorem A: *The external potential $V_{ext}(r)$ is uniquely determined by the ground state particle density $n(\vec{r})$, to within a constant.*
This theorem is asserting that electron density determines V_{ext} and hence fixes $\hat{H}$. And thus, all the observables are determined uniquely by the electron density $n(\vec{r})$.

Proof:
This can be proved by contradiction. Consider two potentials that differ only by a constant:

$$v_1(r) \neq v_2(r) + const$$

$$\hat{H}_1 = \hat{T} + \hat{V}_{ee} + \hat{V}_{ext} \longrightarrow \Psi \tag{7}$$

$$\hat{H}_2 = \hat{T} + \hat{V}_{ee} + \hat{V'}_{ext} \longrightarrow \Psi' \tag{8}$$

By regular variational principle:

$$E_0 = \langle \Psi | \hat{H} | \Psi \rangle < \langle \Psi' | \hat{H} | \Psi' \rangle$$
$$E_0 < \langle \Psi' | \hat{H} - \hat{H}' | \Psi' \rangle + \langle \Psi' | \hat{H}' | \Psi \rangle$$

The last term is E'_0. Subbing in our above definitions of the Hamiltonian to reduce the first term. If we assume $n'(r) = n(r)$ and note that: $E_{ext} = \langle \Psi | \hat{V}_{ext} | \Psi \rangle = \int n(\vec{r}) \hat{v}_{ext} d\vec{r}$
We get:

$$E_0 < E'_0 + \int n(\vec{r})[v_{ext} - v'_{ext} d\vec{r}]$$

We can exchange these hamiltonians $H' \Leftrightarrow H$ to get:

$$E'_0 < E_0 + \int n(\vec{r})[v_{ext} - v'_{ext} d\vec{r}]$$

Adding these last two equations:

$$E_0 + E'_0 < E'_0 + E_0$$

Which is a contradiction that proves only a unique $n(\vec{r})$ exists to define the ground state, or equivalently there cannot exist two potentials (differing by a constant) which lead to the same ground state density.

Theorem B: *An energy functional E[n] exists, such that the exact ground state energy is given by the global minimum of E[n], and the ground state density is the density that minimizes E[n].*
This is an equivalent to the variational theorem, but applied to an electron density defined system. We can state that for a trial $n(r)$ (that satisfies the conditions above [39][40]) , the energy it yield will be an upper bound to the true ground state energy E_0. This allows us to 'search' for our ground state energy, as with any other quantum system.

Proof:
Given that from the first theorem we know a density determines a unique potential, Hamiltonian, and wavefunction. This leads quickly to an equation that can use the conventional variational theorem:

$$E'[n] = \langle \Psi' | \hat{H} | \Psi' \rangle = E_{int}[n] + \int n'(r) v_{ext}(r) dr \leq E_0$$

Our search can now be carried out over densities. Renaming $E_{int} \rightarrow F[n]$ to fit standard nomenclature,

$$E_0 = min_n(F[n] + \int v_{ne}(r) n(r) dr) \tag{9}$$

Now we can move forward with a total energy functional in the form:

$$E[n] = F[n] + \int v_{ne}(r) n(r) dr \tag{10}$$

A1.3 FHI-AIMS Computational Parameters

A1.4 Computational Parameters in FHI-AIMS

The DFT software FHI-AIMS is operated by submitting both a geometry.in that outlines the atomic positions, and a control.in file that defines the parameters for solving the Kohn Sham equations via the Self-Consistency method. I will give a very brief overview on computational parameter that will be mentioned later on.

A1.4.1 Pulay Mixing

Pulay mixing accelerates and stabilizes the self consistency cycle by updating the electron density via a linear combination of previous densities. The residual error is defined as

$$Error(i) = n(i) - n(i-1),$$

where i is the iteration number. The new density is constructed as

$$n^{\text{new}} = \sum_i a_i \, n(i),$$

with the coefficients k_i chosen to minimize $Error(i)$. In addition, a charge mixing parameter, α, is introduced to control the fraction of the update, ensuring stable convergence. The choice of α is highly dependent on the system.

A1.4.2 Collinear Spin Simulations

In collinear spin simulations the total electron density is separated into spin-up and spin-down components:

$$n(\mathbf{r}) = n_\uparrow(\mathbf{r}) + n_\downarrow(\mathbf{r}).$$

The Kohn–Sham equations separate into two sets:

$$(-\frac{1}{2}\nabla^2 + v^{\sigma}_{\text{eff}}(\mathbf{r}))\psi^{\sigma}_i(\mathbf{r}) = \epsilon^{\sigma}_i\, \psi^{\sigma}_i(\mathbf{r}), \quad \sigma = up,\ down$$

with the effective potential for each spin given by

$$v^{\sigma}_{eff}(r) = v_{ext}(r) + v_H[n](r) + v^{\sigma}_{xc}[n_{\uparrow}, n_{\downarrow}](r).$$

A1.5 Computational Approximations in FHI-AIMS

A1.5.0.1 Pseudo-Potentials

Near the atomic centre the Coulomb force is very large, to compensate the any kinetic energy components must be very large. This requires a high rate of oscillations making it costly to represent.Electrons close to the atoms centre contribute very little to the dynamics of the molecule. We can take the core electrons to have the same distribution as an isolated atom. The interaction between inner and outer electrons can be approximated with a mean-field or 'Pseudo-Potential'. The inner electrons can now be cut out of the simulation entirely.

A1.5.0.2 Cut-off Energies:

To shed computational effort DFT packages use cut-off energies. These arise from the fact that higher energies eigenvalues are less likely to be useful in finding the ground state. The cut-off energy depends heavily on the system.
A cut-off energy too low can prevent convergence, or omit potentially important eigen-states.

$$\frac{\hbar^2|\mathbf{k}|^2}{2m} \leq E_{\text{cut}} \longrightarrow |\mathbf{k}| \leq \sqrt{\frac{2mE_{\text{cut}}}{\hbar^2}}$$

A1.5.1 Hellman-Feynman Forces:

The Hellmann-Feynman force greatly simplifies force calculations in quantum mechanics and density-functional theory (DFT) as it describes the classical electrostatic interactions between nuclei and the electron density. It avoids the need to calculate the small change in the wavefunction due to nuclear movement. It is used in geometry optimization.

$$F_n = -\frac{\partial E}{\partial R_n} = -\langle \Psi \left| \frac{\partial H}{\partial R_n} \right| \Psi \rangle.$$

Here:

- F_n is the force on nucleus n.
- $H(R)$ is the electronic Hamiltonian, which depends on the nuclear positions $\mathbf{R}$.

Appendix A2

Results Appendix

A2.1 Cobalt-Porphyrin Projected Density of States

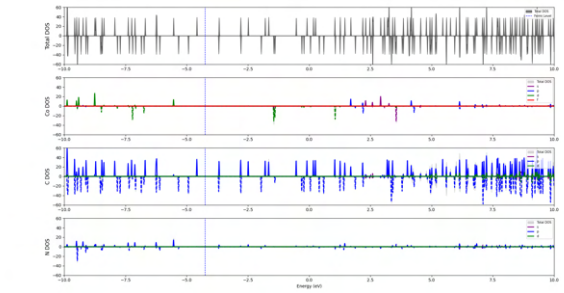

Figure A2.1: PDOS of Co-DPP Molecule

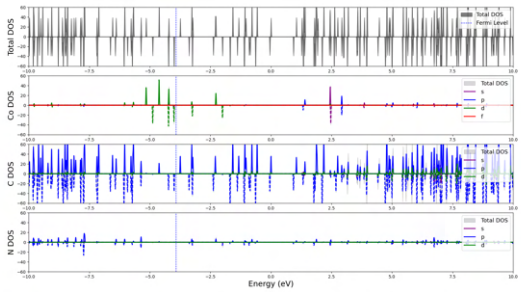

Figure A2.2: PDOS of Co-TPP Molecule

A2.2 Cobalt-Chain Extra Strongly Coupled - PDOS

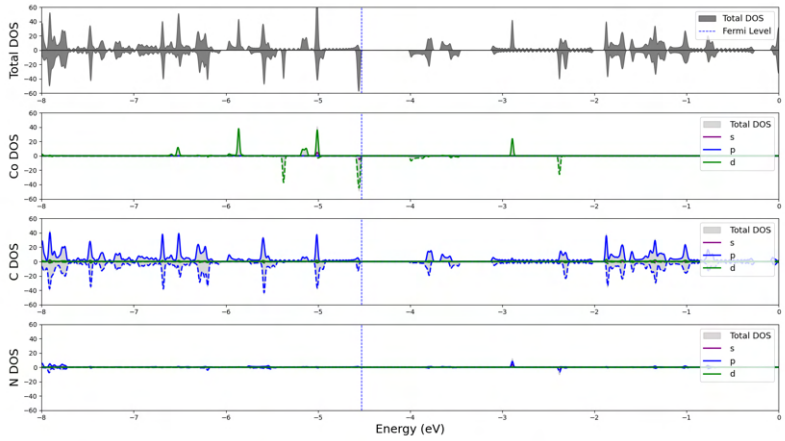

Figure A2.3: Co-Extra Strongly Coupled Network

A2.3 References

Bibliography

[1] Sun, Q., Mateo, L. M., Robles, R., Ruffieux, P., Lorente, N., Bottari, G., Torres, T., Fasel, R. (Year). Inducing open-shell character in porphyrins through surface-assisted phenalenyl extension.

[2] Makino, M., Aihara, J. (2012). Macrocyclic aromaticity of porphyrin units in fully conjugated oligoporphyrins. *The Journal of Physical Chemistry A*, 116(30), 7362–7370.

[3] Wikipedia contributors. (n.d.). Functional derivative. Wikipedia, The Free Encyclopedia. Retrieved March 27, 2025.

[4] Szabo, A. (1996). *Modern quantum chemistry: Introduction to advanced electronic structure theory* (Vol. 1). Dover Publications.

[5] Koch, W., Holthausen, M. C. (2001). *A chemist's guide to density functional theory* (2nd ed.). Wiley-VCH Verlag GmbH.

[6] Sena, A. M. P. (2010). Density functional theory studies of surface interactions and electron transfer in porphyrins and other molecules (Doctoral thesis, University College London). UCL Discovery.

[7] Toulouse, J. (2019, September). European Summerschool in Quantum Chemistry (ESQC). Presentation at the European Summerschool in QuantumChemistry, Sicily, Italy. `https://www.lct.jussieu.fr/pagesperso/toulouse/presentations/presentation_esqc_19.pdf`

[8] Blum, V., Gehrke, R., Hanke, F., Havu, P., Havu, V., Ren, X., Reuter, K., Scheffler, M. (2009). Ab initio molecular simulations with numeric atom-centered orbitals. *Computer Physics Communications*, 180(11).

[9] Harrison, N. M. (n.d.). An introduction to density functional theory. Department of Chemistry, Imperial College of Science Technology and Medicine, London, and CLRC, Daresbury Laboratory, Warrington.

[10] Gao, F., Menchón, R. E., Garcia-Lekue, A., & Brandb, M. (Year). Tunable spin and conductance in porphyrin graphene nanoribbon hybrids. *Journal Name*, Volume(Issue), Page Range.

[11] Kempt, R. (Year). aimstools: A collection of scripts for handling FHI-aims calculations. Retrieved from `https://github.com/romankempt/aimstools`

[12] FHI-aims Team. (2023). *Fritz Haber Institute ab initio materials simulations: FHI-aims All-Electron Electronic Structure Theory with Numeric Atom-Centered Basis Functions—A Users' Guide*. Retrieved from `https://fhi-aims.org/who-we-are`

[13] University of Wisconsin. (n.d.). Molecular Orbital Theory (M9Q5-6). In *Chem 103/104 Resource Book*. Retrieved March 27, 2025, from `https://wisc.pb.unizin.org/minimisgenchem/chapter/molecular-orbital-theory-m9q5-6/`